Nicotinamide Riboside Mitigates Retinal Degeneration by Suppressing Damaged DNA-Stimulated Microglial Activation and STING-Mediated Pyroptosis

Shanshan Zhu,[1,2] Lusi Zhang,[1,2] Ping Tong,[1,2] Jiawei Chen,[1,2] Cong Wang,[1,2] Zewei Wang,[1,2] Jingyuan Liu,[1,2] Peiyun Duan,[1,2] Qian Jiang,[1,2] Yubing Zhou,[1,2] Guangshuang Tan,[1,2] Xian Zhang,[1,2] and Bing Jiang[1,2]

[1]Department of Ophthalmology, The Second Xiangya Hospital of Central South University, Changsha, Hunan, China
[2]Hunan Clinical Research Center of Ophthalmic Disease, Changsha, China

Correspondence: Bing Jiang, Department of Ophthalmology, The Second Xiangya Hospital of Central South University, No.139, Renmin Middle Rd., Changsha, Hunan 410011, China; drjiangb@csu.edu.cn.
Xian Zhang, Department of Ophthalmology, The Second Xiangya Hospital of Central South University, No.139, Renmin Middle Rd., Changsha, Hunan 410011, China; xianz0707@csu.edu.cn.

XZ and BJ contributed equally to this work.

Received: October 11, 2024
Accepted: March 10, 2025
Published: April 7, 2025

Citation: Zhu S, Zhang L, Tong P, et al. Nicotinamide riboside mitigates retinal degeneration by suppressing damaged DNA-stimulated microglial activation and STING-mediated pyroptosis. *Invest Ophthalmol Vis Sci.* 2025;66(4):14. https://doi.org/10.1167/iovs.66.4.14

Purpose. Microglial activation plays a pivotal role in the pathogenesis of retinal degeneration, contributing to neuroinflammation within the retina. Previous studies identified that nicotinamide riboside (NR) mitigated light-induced retinal degeneration (LIRD) and inhibited microglial activation. The cGAS-STING signaling pathway has been recognized as a key mediator of inflammation in response to cellular stress and tissue damage. This study further explores the regulatory impact of NR on microglial activation and STING-mediated pyroptosis in retinal degeneration.

Methods. Balb/c mice were subjected to bright light exposure to induce retinal degeneration. Bioinformatics analysis was used to identify the upregulated key genes and signaling pathways involved in the progression of retinal degeneration, based on mouse transcriptomes from the LIRD model. Molecular biology techniques and immunofluorescence staining were used to assess cGAS-STING activation and expression of pyroptosis-associated molecules. Retinal function, photoreceptor apoptosis and inflammatory response were evaluated in the presence and absence of NR supplementation.

Results. Exposure to bright light resulted in mitochondrial dysfunction and the release of dsDNA, significantly triggering the activation of cGAS-STING pathway and microglial pyroptosis. In contrast, NR treatment preserved mitochondrial biosynthesis, inhibited STING expression in reactive microglia, and dampened the pro-inflammatory response. Additionally, intraperitoneal administration of the STING inhibitor H151 reduced light-induced microglial activation and pyroptosis, while improving retinal function and promoting photoreceptor survival.

Conclusions. These findings suggest that NR confers neuroprotection by attenuating damaged DNA-triggered STING-mediated microglial activation and pyroptosis. Targeting the cGAS-STING pathway presents a promising therapeutic avenue for retinal degeneration.

Keywords: fundus autofluorescence, protoporphyrin IX, choroid

Photoreceptor degeneration is a hallmark of various vision-threatening disorders, including AMD and RP,[1,2] with inflammation and microglial activation playing a crucial role.[3,4] Pyroptosis, a form of inflammatory cell death, is linked to microglial activation processes.[5,6] Inflammatory stimuli activate the inflammasome, leading to caspase-1 activation, gasdermin D (GSDMD) cleavage, and lytic cell death.[7,8] This process also releases proinflammatory cytokines, further promoting inflammation and accelerating vision loss.[3,9] Thus, targeting retinal inflammation is a promising therapeutic strategy.

The visual process demands substantial energy, primarily derived from oxidative metabolism linked to ATP synthesis.[10] Mitochondria, which are essential for cellular energy production, are particularly vulnerable to oxidative stress.[11,12] Mitochondrial dysfunction is a key characteristic of retinal degenerative diseases.[13] Under stress conditions, damaged mitochondria release reactive oxygen species (ROS) and mitochondrial DNA (mtDNA),[14] activating the cGAS-STING pathway,[15] which triggers an immune response. The cGAS-STING pathway has been implicated in neuroinflammation and retinal degeneration, particularly in AMD, making it a potential target for therapy.[16,17]

The nicotinamide adenine dinucleotide (NAD^+) is a critical metabolic intermediate in maintaining mitochondrial homeostasis and genome integrity.[18] Emerging evidence has identified that maintenance NAD^+ levels is critical to retinal health. Mutations in nicotinamide mononucleotide

Investigative Ophthalmology & Visual Science

adenylyltransferase-1 (NMNAT1), a NAD^+ salvage pathway enzyme, causes Leber congenital amaurosis type 9 (LCA9).[19] Lin and colleagues[20] found that retinal NAD^+ levels decline in models of retinal degeneration, and mice made deficient in NAMPT had diminished retinal NAD^+ and developed retinal degeneration. Further, they demonstrated that systemic treatment with the NAD^+ precursor nicotinamide mononucleotide was protective in mouse models of retinal degeneration.[21] Nicotinamide riboside (NR) is a key intermediate in the biosynthesis of NAD^+. Our recent findings demonstrated that NR administration increased NAD^+ levels in the retinas, suppressed microglial activation and provided protection against photoreceptor cell damage in rodent models of light-induced retinopathy.[22] However, the role of NR in modulating neuroinflammation and microglial activation is still under investigation.

The substantial activation of the cGAS-STING pathway has been observed in the retinas of mice exposed to light damage.[23] This study demonstrated that cGAS and STING were predominantly expressed and upregulated in retinal microglia during degeneration. Moreover, NR administration effectively reduced STING expression in reactive microglia after light-induced retinal damage. Inhibiting STING expression significantly curtailed microglial pyroptosis and improved retinal function, highlighting a potential therapeutic approach for retinal degenerative diseases.

Material and Methods

Animals

This study used eight-week-old male BALB/c mice (Hunan SJA Laboratory Animal Company, Changsha, Hunan, China). All procedures adhered to the ARVO Statement for the Use of Animals in Ophthalmic and Vision Research and were approved by the Institutional Animal Care and Use Committee of the Second Xiangya Hospital of Central South University.

Animal Model and Drug Administration

The method for inducing light-induced retinal degeneration (LIRD) has been described previously.[22] NR chloride (Cat. no. A111004, CAS no. 23111-00-4; Zhengzhou Alpha Chemical Co., Ltd., Zhengzhou, China) was diluted in PBS. Balb/c mice were given intraperitoneal injections of either PBS or NR (1000 mg/kg) at a volume of 10 µL per gram of body weight. Two injections were administered before bright light exposure: the first at 6:00 PM the day before, and the second at 9:00 AM on the day of light insult. The STING inhibitor H151 (MCE, Cat no. HY-112693) was diluted in PBS with 5% Tween 80 and 40% polyethylene glycol 300. Mice were administered intraperitoneal injections of H151 (15 mg/kg) or vehicle, with injections given before and 24 hours after bright light exposure. Pan-caspase inhibitor Z-VAD-FMK (Sellect, CAS: 187389-52-2) was dissolved in dimethyl sulfoxide to yield a 10 mM stock solution. Before administration, Z-VAD-FMK was diluted in 95% corn oil. Mice received one intraperitoneal injection of Z-VAD-FMK (10 mg/kg) or vehicle the day before toxic light exposure.

ERGs

After overnight dark adaptation, mice were anesthetized via intraperitoneal injection of 1% sodium pentobarbital (8 mL/kg; Sigma-Aldrich Corp., St. Louis, MO, USA). After pupil dilation, round metal electrodes were placed on the center of the cornea, with the reference electrode positioned under the skin at the bregma and the ground electrode embedded in the middle of the tail. Electrical signals were recorded using the ERG (RetiMINER System; AiErXi Medical Equipment Co., Ltd, Chongqing, China). The ERG measurement results of both eyes from one mouse were averaged to represent a single sample.

Immunofluorescence and Quantification

Mouse eyes or dissected retinas were fixed in 4% paraformaldehyde (PFA). Eyeballs were dehydrated in gradient sucrose and cut at 30-µm thickness using a Leica CM1950 cryostat (Leica, Weztlar, Germany). The retinas or sections were rinsed with PBST (PBS with 0.1% Triton X-100) and blocked in PBST containing 3% bovine serum albumin for 1 hour at room temperature. The corresponding primary antibodies and secondary antibodies were listed in Table 1. The slides were covered with mounting medium (Sigma-Aldrich Corp.). Retinal immunostaining was captured using an Axio Imager M2 fluorescence microscope (Carl Zeiss, Oberkochen, Germany). The number of marker-positive microglia cells was counted manually using the Cell Counter plugin in ImageJ. The cell count for each retinal layer was calculated separately.

Transmission Electron Microscopy (TEM)

The retina was extracted under a microscope and quickly divided into $1 \times 1 \times 3$ mm^3 tissue pieces. Then the tissue was placed in an electron microscope fixing solution (Merck Millipore, MA, USA). Following dehydration in acetone, the tissue was embedded, sectioned and stained. Images were captured with a HT7700 transmission electron microscope (Hitachi, Japan). Systematic ImageJ Analysis for TEM Measurements of Organelle Morphology were previously described.[24] Briefly, open TEM images in *ImageJ*, with the appropriate scale set and the measurement column configured in the settings. Freehand Selections traced the outline of the cell and mitochondrial membranes (Supplementary Fig. S1A). The Cell Counter plugin was used to count the number of mitochondria in the selected regions (Supplementary Fig. S1B). For cristae morphology analysis, each image was divided into four quadrants, and two randomly selected quadrants were analyzed for consistency across all images. The Cell Counter plugin was used to count the number of cristae within the chosen quadrants (Supplementary Fig. S1C). Cristae morphology scoring was performed by assigning a score between 0 and 4 based on the number and appearance of cristae: 0 for no sharply defined crista, 1 for more than 50% of the mitochondrial area lacking cristae, 2 for more than 25% of mitochondrial area lacking cristae, 3 for many cristae (over 75% of area) but irregular, 4 for many regular cristae.

TUNEL Assay

Mouse eyeballs were sectioned at 14-µm thickness, and cell death was detected using the In Situ Cell Death Detection Kit, Fluorescein (Roche, Basel, Switzerland, CAS#7791-13-1) according to the manufacturer's protocol. Briefly, the prepared sections were fixed with 4% PFA and washed three times in PBS. They were then permeabilized with

Investigative Ophthalmology & Visual Science

Table 1. Antibodies for Immunofluorescence

Protein Target	Host Species	Dilution	Manufacturer	Catalogue Number
Iba-1	Rabbit	1:500	Abcam*	ab178846
Iba-1	Goat	1:800	Abcam*	ab5076
CD68 (FA-11)	Rat	1:200	Thermo†	14-0681-82
dsDNA	Mouse	1:200	Santa Cruz‡	sc-58749
Tom20 (D8T4N)	Rabbit	1:200	Cell Signaling Technology§	42406
Cgas	Mouse	1:200	Santa Cruz‡	sc-515777
STing	Rabbit	1:200	Proteintech‖	19851-1-AP
NLRP3	Rabbit	1:200	Abmart¶	P60622R3
Casepase-1	Mouse	1:100	Santa Cruz‡	sc-56036
IL-1β	Mouse	1:100	Cell Signaling Technology§	12242
GSDMD	Mouse	1:200	Santa Cruz†	sc-393581
Goat Anti-Rabbit IgG H&L (Alexa Fluor 488)	Goat	1:400	Jackson#	111-545-003
Goat Anti-Rat IgG H&L (Alexa Fluor 594)	Goat	1:300	Jackson#	112-505-175
Donkey Anti-Rabbit IgG H&L (Alexa Fluor 488)	Donkey	1:400	Thermo†	A21206
Donkey Anti-Mouse IgG H&L (Alexa Fluor 555)	Donkey	1:400	Thermo†	A31570
Donkey Anti-goat IgG H&L (Alexa Fluor 568)	Donkey	1:400	Thermo†	A11057

* Abcam, Cambridge, MA, USA.
† Thermo Fischer Scientific, Waltham, MA, USA.
‡ Santa Cruz Biotechnology, Dallas, TX, USA.
§ Cell Signaling Technology, Danvers, MA, USA.
‖ Proteintech, Rosemont, IL, USA.
¶ Abmart, Berkeley Heights, NJ, USA.
# Jackson Laboratories, Bar Harbor, ME, USA.

0.5% Triton-X100, washed once in PBS, and incubated in the premixed working buffer for 1 hour at 37 °C in the dark.

Quantitative Real-Time PCR (qPCR) Analysis

Total RNA was isolated from retinal tissues using TRIzol reagent (Invitrogen, San Diego, CA, USA), following the manufacturer's protocol. CDNA was synthesized using the RevertAid Master Mix (Thermo Fisher Scientific, Waltham, MA, USA). QPCR was conducted on an Applied Biosystems StepOne Plus Real-Time PCR System (Thermo Fisher Scientific) with TB Green Premix Ex Taq II (RR820A; TaKaRa Bio. Co., Shiga, Japan). The β-actin served as the internal control. The primers for qPCR are listed in Table 2. Gene expression levels were quantified using the $2^{-\Delta\Delta Ct}$ method.

RNA Sequencing and Bioinformatics Analysis

Total RNA was extracted from mouse retinas. Paired-end libraries were prepared using a ABclonal mRNA-seq Lib Prep Kit (ABclonal, Woburn, MA, USA) following the manufacturer's instructions. PCR products were purified (AMPure XP system; Beckman Coulter, Inc, Southfield, MI, USA) and library quality was assessed on an Agilent Bioanalyzer 4150 system (Agilent Technologies, Winooski, VT, USA). Finally, sequencing was performed with a 6000/MGISEQ-T7 instrument. The data generated from Illumina/BGI platform were used for bioinformatics analysis. Then clean reads were separately aligned to reference genome with orientation mode using HISAT2 software to obtain mapped reads. Differential gene expression analysis was conducted using the DESeq2 R package, with a significance threshold of $Q < 0.05$ and a fold change > 1.5. GO function enrichment and Kyoto Encyclopedia of Genes and Genomes (KEGG) pathway enrichment analysis were carried out using the clusterProfiler R software package.

Table 2. Primer Sequences for qPCR

Gene	Primer Sequence (5′–3′)
PGC1α	Forward: AAGTGTGGAACTCTCTGGAACTG
	Reverse: GGGTTATCTTGGTTGGCTTTATG
TFAM	Forward: GTTTGTTGTGTGTGGGTGCTCTG
	Reverse: CTGTCTGCGAAGGGCCATCC
mtDNA	Forward: AGTCGGCATCGTTTATGGTC
	Reverse: CGCGGTTCTATTTTGTTGGT
SIRT1	Forward: TGTGAAGTTACTGCAGGAGTGTAAA
	Reverse: GCATAGATACCGTCTCTTGATCTGAA
UPC2	Forward: GCTGGTGGTGGTCGGAGATAC
	Reverse: TACGGGCAACATTGGGAGAAGTC
UPC3	Forward: ATCGCCAGGGAGGAAGGAGTC
	Reverse: AGGTCACCATCTCAGCACAGTTG
cGAS	Forward: GGAAGGAACCGGACAAGCTA
	Reverse: AACTCCGACTCCCGTTTCTG
STing	Forward: TCCCTGCTCTCTGTTGACCTGTG
	Reverse: TGTTCCTTCTCCCTCTCGCCATC
NLRP3	Forward: CTTCTAGCTTCTGCCGTGGTCTCT
	Reverse: CGAAGCAGCATTGATGGGACA
Caspase-1	Forward: GTACACGTCTTGCCCTCATTATCTG
	Reverse: TTTCACCTCTTTCACCATCTCCAG
GSDMD	Forward: TTGAAGGGTGAAGGCAAG
	Reverse: AGCCAATAAGCAGTTGGG
IL 1β	Forward: GCAACTGTTCCTGAACTCAACT
	Reverse: ATCTTTTGGGGTCCGTCAACT
IL-18	Forward: GGAGGGTTTGTGTTCCAG
	Reverse: AATACAGGCGAGGTCATCA
TNF-α	Forward: ACGGCATGG ATCTCAAAGAC
	Reverse: AGATAGCAAATCGGCTGACG
IL-6	Forward: GTTCTCTGGGAAATCGTGG
	Reverse: CTGCAAGTGCATCATCGTT
NF-κB	Forward: CTGCACTCTATGGCTCAGG
	Reverse: GGGACAGCGACACCTTT
β-actin	Forward: CACGATGGAGGGGCCGGACTCATC
	Reverse: TAAAGACCTCTATGCCAACACAGT

Statistical Analyses

Statistical analyses were conducted using GraphPad Prism 9.0.0 (GraphPad Software, La Jolla, CA, USA, www.graphpad.com). An unpaired *t*-test was used to assess significant differences between two treatment groups, while one-way or two-way ANOVA with Tukey's multiple comparisons test was applied for multiple comparisons. Statistical significance was set at $P < 0.05$. All results are presented as mean ± SEM, with n representing the number of animals per group.

Results

NR Protected Against Light-Induced Photoreceptor Apoptosis and Suppressed Microglial Activation

Apoptosis is a key feature of retinal degeneration, driving photoreceptor loss and visual impairment.[25] In our study, apoptotic signals were observed as early as 1 day post-light exposure, peaking at day 3 and declining through days 5 and 7 (Figs. 1A, 1B). Transcriptomic analysis of mouse

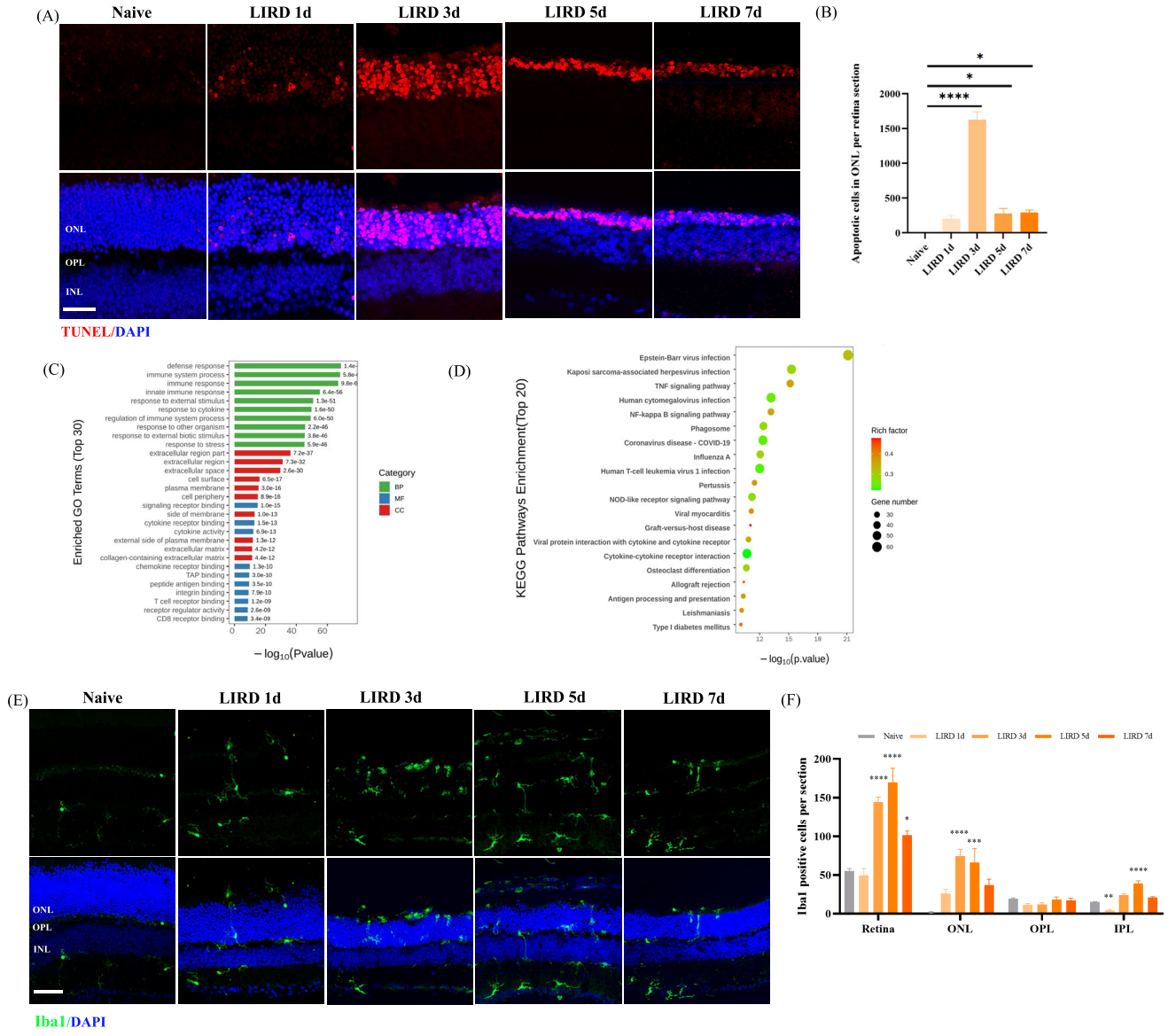

Figure 1. Photoreceptor apoptosis and microglial activation in the LIRD mouse model. **(A)** Apoptotic cells in the ONL were identified by TUNEL staining. Representative images of apoptotic cells in frozen retinal sections at one, three, five, and seven days after light exposure. *Scale bar*: 30 µm. **(B)** Statistical graph of TUNEL positive cells in ONL of each group (n = 4–6/group). **(C)** Gene ontology (GO) enrichment analysis of the top 30 DEGs ranked by *P* value. BP, Biological process; MF, molecular function; CC, cellular component. **(D)** KEGG pathway enrichment analysis of the DEGs. Rich factor represents the ratio of the number of enriched DEGs in the KEGG category to the total genes in that category. **(E)** Activated microglia and cell nuclei were identified using Iba1 and DAPI staining, respectively. Representative images showing microglial activation at one, three, five, and seven days after light exposure. *Scale bar*: 50 µm. **(F)** Quantification of Iba1-positive cells across the whole retina, ONL, OPL and IPL at different time points after light exposure (n = 6/group). *$P < 0.05$, **$P < 0.01$, ***$P < 0.001$, ****$P < 0.0001$ versus naive group by one-way ANOVA with Tukey's multiple comparisons test. *Error bars*: SEM.

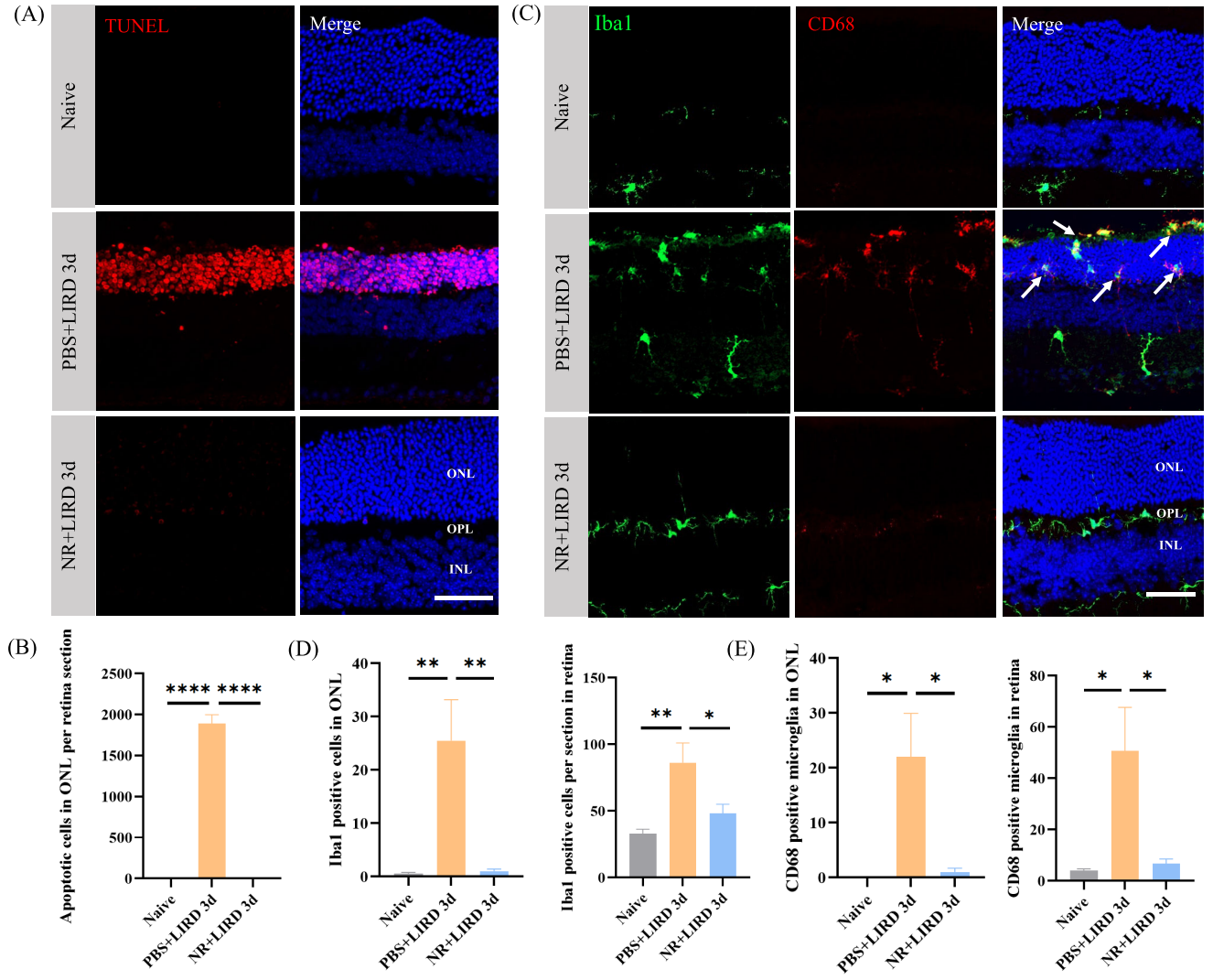

Figure 2. NR treatment inhibited apoptosis and microglial activation in the LIRD mouse model. **(A)** Representative morphologic images of each group, with TUNEL (red) labeling apoptotic cells and DAPI (*blue*) staining cell nuclei. *Scale bar*: 50 µm. **(B)** Quantification of TUNEL-positive nuclei in the ONL, counted from the entire retina ($n = 5$–6/group). Mice treated with NR exhibited significantly fewer TUNEL-positive cells compared to the PBS-treated group. **(C)** Representative images of Iba1-positive and CD68-positive (phagocytic microglia marker) cells in naive, PBS+LIRD3d, and NR+LIRD3d groups. *Scale bar*: 50 µm. **(D)** Quantification of Iba1-positive cells and **(E)** CD68-positive cells in both ONL and whole retina for each group at three days after light exposure ($n = 4$/group). NR treatment significantly suppressed microglia activation, compared with the PBS-treated group ($n = 4$/group). $^{*}P < 0.05$, $^{**}P < 0.01$, $^{****}P < 0.0001$ by one-way ANOVA with Tukey's multiple comparisons test.

retinas 24 hours after light exposure identified 2,303 differentially expressed genes (DEGs), including 1494 upregulated and 809 downregulated genes (Supplementary Fig. S2). GO analysis linked these DEGs to immune response activation (Fig. 1C), whereas KEGG analysis highlighted TNF and NF-κB pathways (Fig. 1D).

Microglia play a pivotal role in the innate immune response during neuroinflammation associated with retinal degenerative diseases. Microglial activation was detected as early as 1 day post-light exposure, with activated microglia migrating to the outer nuclear layer (ONL), the site of degeneration (Fig. 1E). The activation peaked at day 3, coinciding with the progression of photoreceptor apoptosis. Additionally, we quantified the number of activated microglia in both the outer plexiform layer (OPL) and inner plexiform layer (IPL) after light exposure (Fig. 1F). Microglial activation in the IPL exhibited a temporal progression similar to that observed in the entire retina and ONL, suggesting a potential association between these microglia and the retinal degenerative process.

To assess NR's effect on retinal apoptosis and microglial activation, mice were pretreated with NR and assessed three days after light exposure. As shown in Figures 2A and 2B, NR robustly inhibited photoreceptor apoptosis in the LIRD mice. Quantitative analysis of microglial presence in the ONL and across the entire retina revealed that NR treatment substantially reduced both total microglia and CD68+ microglia (Figs. 2C–E). The pan-caspase inhibitor Z-VAD-FMK also reduced apoptosis and microglial activation, but not as effectively as NR (Supplementary Fig. S3), suggesting that NR's effects extend beyond apoptosis inhibition, likely modulating upstream signaling to reduce inflammation. Collectively, these results suggest that NR administration effectively mitigates photoreceptor apoptosis and

Investigative Ophthalmology & Visual Science

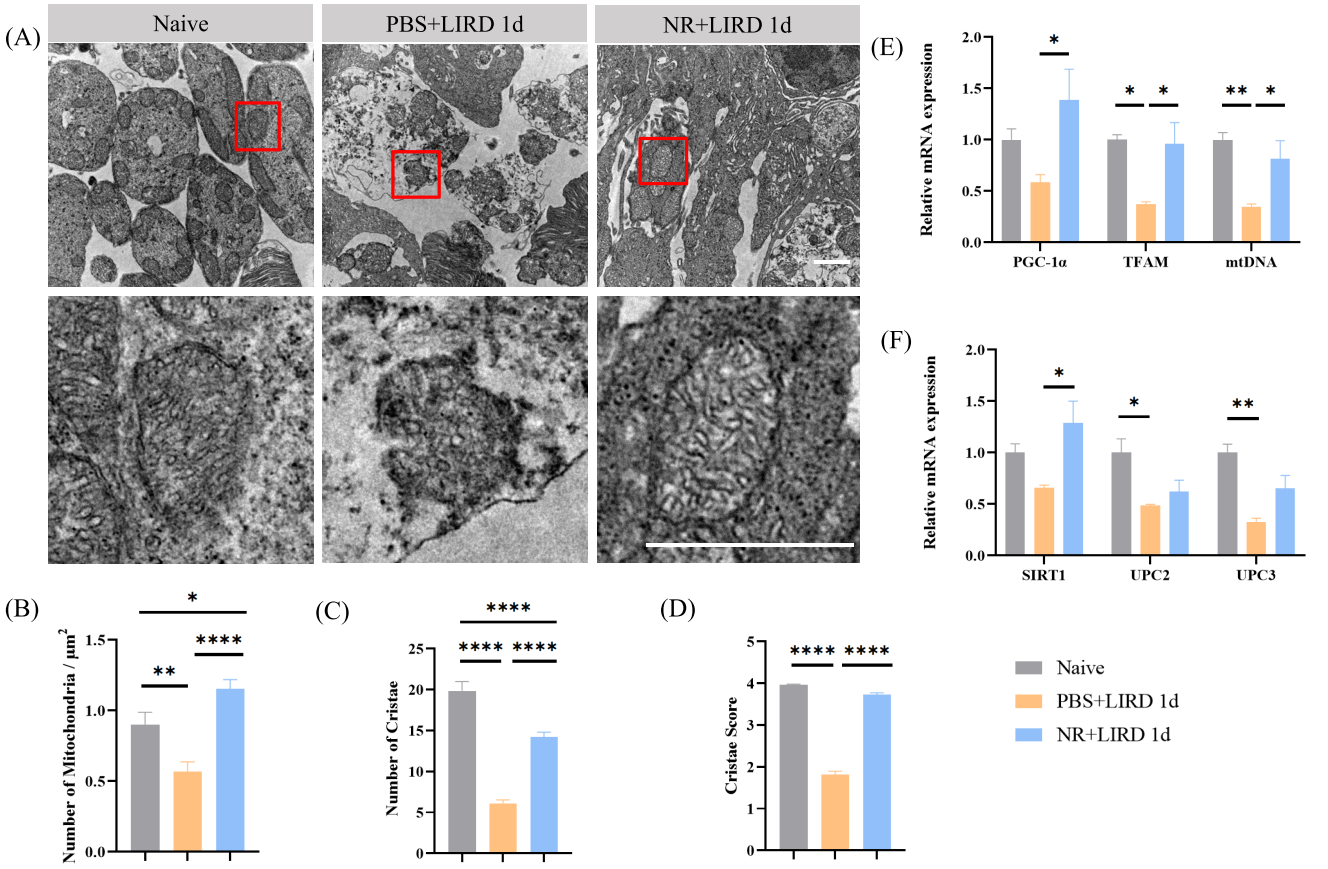

Figure 3. NR treatment retained mitochondrial integrity and enhanced mitochondrial biogenesis in the LIRD mice. **(A)** Representative TEM images of mitochondria (*upper panels*; indicated magnification: 10kx.). Magnified images of single mitochondria from each group (*lower panels*). *Scale bar*: 1 µm. **(B)** Number of mitochondria per square micrometer (10–15 images per group). **(C)** Quantification of cristae number and **(D)** cristae score. 117–239 mitochondria per group. **(E)** QPCR analysis for PGC-1α, TFAM, mtDNA, and **(F)** SIRT1, UPC2 and UPC3 expression in naive, PBS + LIRD1d, and NR+LIRD1d groups (n = 4/group). *P < 0.05, **P < 0.01, by one-way ANOVA with Tukey's multiple comparisons test.

microglial activation in response to light-induced retinal injury.

NR Preserved Mitochondrial Integrity and Enhanced Mitochondrial Biogenesis After Light Exposure

Mitochondrial dysfunction is a common hallmark of retinal degenerative diseases, often preceding microglial activation, neuroinflammation, and subsequent cell death.[26,27] As a key precursor of NAD^+, NR is essential for maintaining mitochondrial function. To elucidate the mechanisms underlying NR's protective effects, mitochondrial structure in mouse retinas was examined 24 hours after light exposure, with or without NR treatment, using electron microscopy. As shown in Figures 3A through 3D, light damage significantly decreased the mitochondria number and disrupted cristae morphology. Specifically, the average number of cristae per mitochondrion and the cristae score were significantly lower in the LIRD group compared to the naive group. NR treatment significantly preserved these structural features, suggesting that NR helps maintain mitochondrial integrity and efficiency.

We further investigated the impact of NR on mitochondrial biogenesis, which plays a crucial role in maintaining mitochondrial function and ensuring energy production capacity.[26] PGC-1α is a master regulator of mitochondrial biogenesis, facilitating the growth and replication of mitochondria. Quantitative qPCR analysis showed that NR treatment significantly upregulated the mRNA expression of PGC-1α, as well as its downstream target gene, mitochondrial transcription factor A (TFAM), which supports mitochondrial replication and mtDNA integrity.[28] Elevated mtDNA levels confirmed enhanced mitochondrial activity (Fig. 3E). SIRT1 is an NAD^+-dependent deacetylase that regulates mitochondrial function and metabolic processes. The significant increase in SIRT1 expression further suggests that NR may improve mitochondrial function and reduce oxidative stress (Fig. 3F). Additionally, NR mitigated the reduction in UCP2 and UCP3 expression induced by light damage (Fig. 3F). These findings indicate that NR enhances mitochondrial health, both functionally and structurally, contributing to retinal protection.

NR Mitigated cGAS-STING Pathway Activation Stimulated by Damaged DNA

Multiple studies have shown that the release of self-DNA, including dsDNA and mtDNA, can activate the cGAS-STING pathway, driving neuroinflammation in neurodegenerative

Investigative Ophthalmology & Visual Science

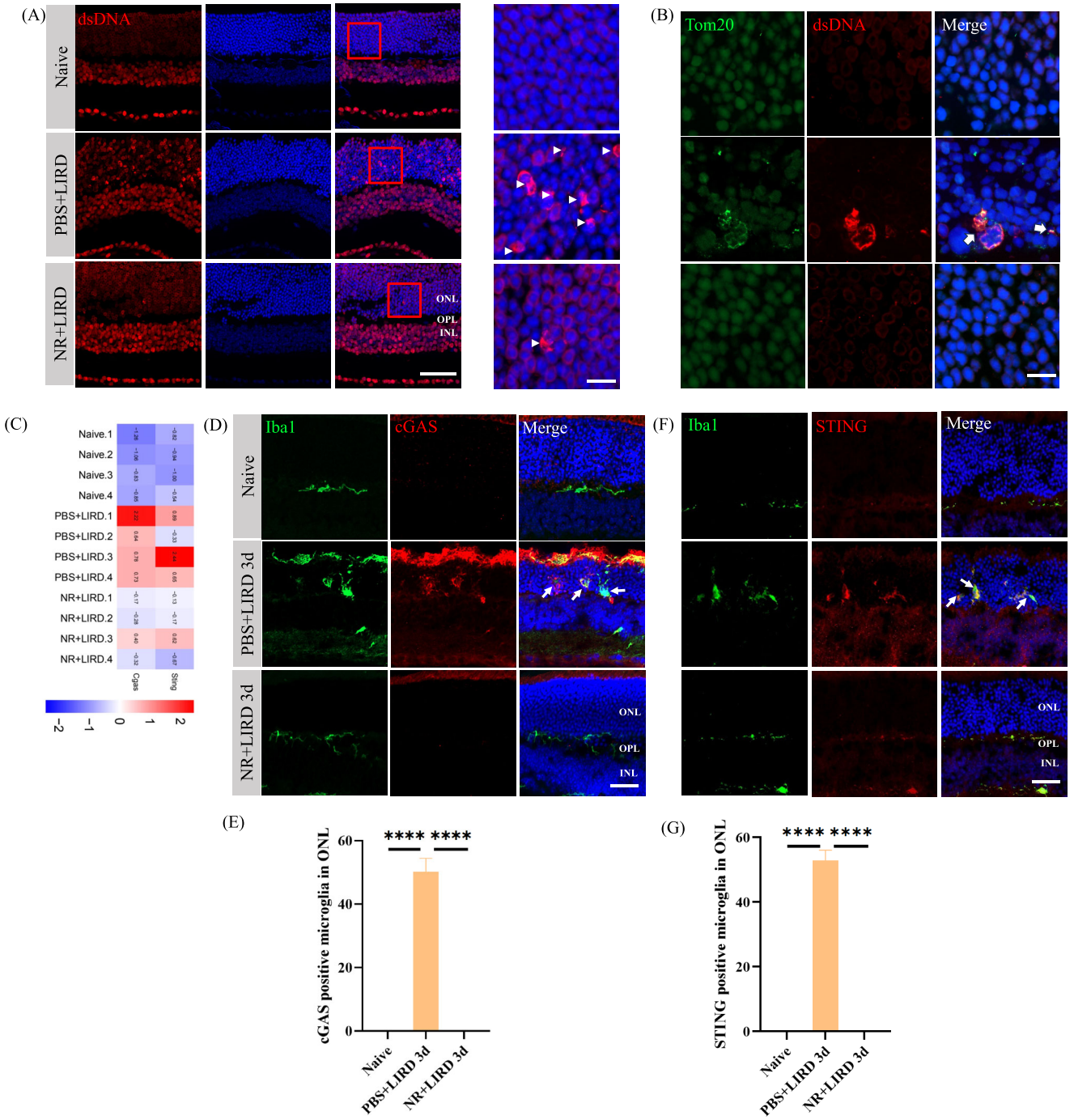

Figure 4. NR mitigated damaged DNA-stimulated cGAS-STING pathway. **(A)** Representative microscopic images of dsDNA immunopositivity (in *red*) and DAPI-counterstained nuclei (in *blue*). *Scale bar*: 50 µm. The boxed areas within the images were magnified and displayed in the right panels (*arrowheads*). *Scale bar*: 10 µm. **(B)** Colocalization of Tom20 (*green*), dsDNA (*red*), and DAPI (*blue*) expressions in retinas of each group (*arrows*). *Scale bar*: 10 µm. **(C)** Heatmap of cGAS and STING from RNA sequencing of naive and LIRD retinas with or without NR treatment (n = 4/group). **(D)** Colocalization of cGAS (*red*) and Iba1-positive microglia (*green*) expression in the retinas of each group (*arrows*). *Scale bar*: 30 µm. **(E)** Quantification of cGAS-positive microglia of each group in the ONL at three days after light exposure (n = 4–6/group). **(F)** Colocalization of STING (*red*) and Iba1-positive microglia (*green*) expression in the retinas of each group (*arrows*). *Scale bar*: 30 µm. **(G)** Quantification of STING-positive microglia of each group in the ONL at three days after light exposure (n = 5–6/group). NR treatment significantly decreased the expression of cGAS and STING compared with the PBS-treated group, ****$P < 0.0001$.

diseases.[29–31] To investigate whether light exposure induces self-DNA release in the retina, we performed immunofluorescence staining on retinal sections. Our results revealed a significant accumulation of dsDNA and mtDNA in the cytoplasm, particularly in the ONL, following light exposure (Figs. 4A, 4B). In contrast, minimal cytoplasmic DNA release was observed in retinas from naive or NR-treated groups, suggesting that NR prevented excessive DNA leak-

age into the cytoplasm. To further assess the activation of the cGAS-STING pathway, we analyzed transcriptomic changes in LIRD mouse retinas. RNA sequencing of LIRD retinas showed increased mRNA expression levels of cGAS and STING compared to naive retinas, with NR treatment significantly attenuating this upregulation (Fig. 4C). These transcriptional findings were further supported by immunofluorescence staining, which revealed markedly increased cGAS and STING protein levels in microglia of LIRD retinas (Figs. 4D–G). Notably, NR treatment significantly reduced cGAS

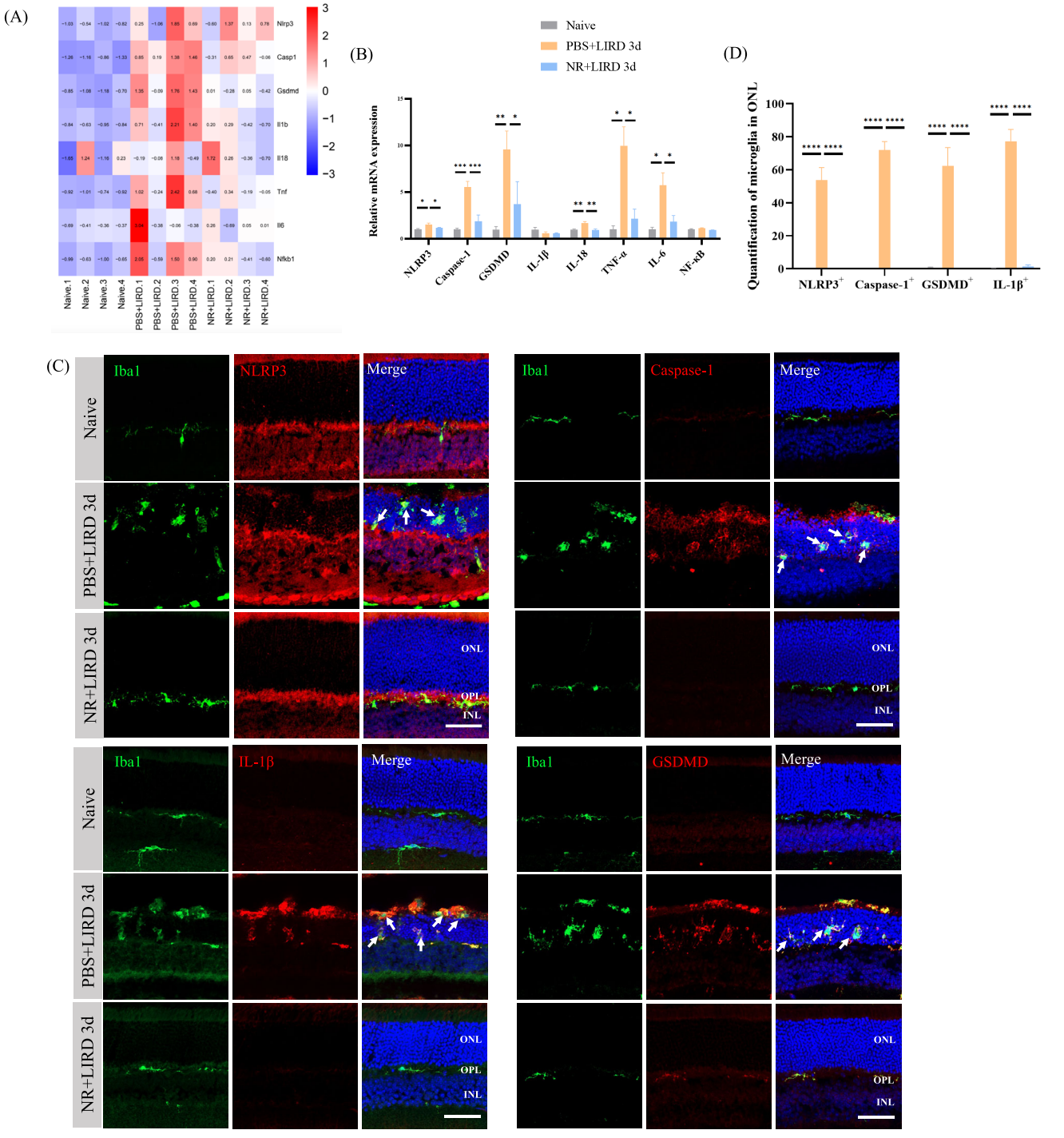

Figure 5. NR inhibited light-induced microglial pyroptosis. **(A)** Heatmap of NLRP3, caspase-1, GSDMD, IL-18, IL-1β, TNF-α, IL-6, and p-NF-κB from RNA sequencing of naive and LIRD retinas with or without NR treatment (n = 4/group). **(B)** The mRNA levels of pyroptosis-associated markers (n = 4–6/group) *P < 0.05, **P < 0.01, ***P < 0.001. **(C)** Colocalization of pyroptosis-related proteins (*red*) and Iba1 + microglia (*green*) in the retina sections in each group (*arrows*). *Size marker*: 50 µm. **(D)** Quantification of NLRP3+, caspase-1+, GSDMD+, and IL-1β+ in Iba1+ cells of each group in ONL at three days after light exposure. NR treatment significantly decreased the expression of pyroptosis-related proteins in the microglia compared with the PBS-treated group (n = 4–6/group). ****P < 0.0001, by one-way ANOVA with Tukey's multiple comparisons test.

Investigative Ophthalmology & Visual Science

and STING expression in microglia, further indicating its role in modulating cGAS-STING signaling under retinal stress conditions. Collectively, these results suggest that NR mitigates light-induced DNA release and the subsequent activation of the cGAS-STING pathway in retinas subjected to light-induced damage.

NR Suppressed Light-Induced Neuroinflammation and Microglial Pyroptosis

Under pathological conditions, degenerated photoreceptors release damaged DNA, which is detected by microglia, initiating neuroinflammation. Microglia recognize various inflammasomes, triggering pyroptosis through surface receptors such as GSDMD and NLRP3, which, in turn, promote the secretion of proinflammatory cytokines like TNF-α and IL-1β via the NF-κB pathway, exacerbating neuroinflammation.[32] Our transcriptomic sequencing analysis revealed an increased expression of genes associated with pyroptosis in retinas following light-induced damage. These genes included NLRP3, caspase-1, GSDMD, as well as downstream pro-inflammatory cytokines such as IL-1β, IL-18, IL-6, TNF-α, and NF-κB (Fig. 5A). This upregulation was further confirmed by qPCR, which showed a significant increase in the mRNA levels of these genes (Fig. 5B). Dual staining of retinal sections with anti-inflammatory cytokine and anti-Iba1 antibodies revealed marked upregulation of pyroptosis-related proteins in microglia of the LIRD group, indicating microglial pyroptosis (Figs. 5C, 5D). This finding is consistent with previous studies identifying pyroptosis predominantly in inflammatory cells, particularly microglia.[33] Notably, NR treatment attenuated these inflammatory responses (Fig. 5D). These findings collectively demonstrate the robust activation of inflammatory responses and pyroptosis in the retina following light-induced damage. Furthermore, NR treatment significantly alleviates microglial pyroptosis, providing evidence of its protective effect in the LIRD mouse model.

NR Prevented Retinal Degeneration by Suppressing cGAS-STING-Mediated Microglial Pyroptosis

Given that STING mediates its effects through the NF-κB pathway, we hypothesized that STING plays a pivotal role in retinal neuroinflammation. To investigate the impact of STING deficiency on light-induced retinal inflammation, the selective STING inhibitor H-151 was administered intraperitoneally to Balb/c mice, followed by a series of measurements three days after light exposure. Our results demonstrate that STING inhibition markedly reduced the number of CD68+ microglia in the retina after light-induced damage (Figs. 6A, 6B). This suggests that STING activation is crucial for microglial recruitment and activation in response to retinal insult. Moreover, H-151 treatment significantly suppressed the expression of pyroptosis-associated proteins in the retinal microglia post-light exposure (Figs. 6C, 6D). ERG analysis revealed significantly preserved retinal function in the H-151-treated group compared to the LIRD group. Specially, NR supplementation did not provide additional benefits beyond the effects of H-151 treatment alone (Figs. 6E, 6F). Altogether, these results indicate that STING inhibition effectively reduces microglial activation, pyroptosis, and retinal dysfunction following light-induced injury. Furthermore, NR's retinal protective effects appear to operate, at least partially, through the suppression of the microglial cGAS-STING pathway, reinforcing its potential therapeutic role in mitigating retinal inflammation and degeneration.

Discussion

We previously reported that systemic delivery of NR significantly increased NAD^+ levels in the retinas of LIRD mice.[22] This study further explores NR's role in neuroinflammation, revealing that it protects against LIRD by inhibiting photoreceptor apoptosis and microglial pyroptosis via the cGAS-STING pathway. STING deficiency reduced microglial activation and proinflammatory chemokines, offering retinal protection.

Our study showed DNA leakage in photoreceptors and cGAS-STING activation after light exposure. The cGAS-STING signaling is a key cytosolic DNA-sensing innate immunity pathway that regulates inflammation and cell apoptosis. Studies indicate that cytoplasmic dsDNA or mtDNA leakage from mitochondrial damage can activate STING.[30,34] Inhibiting cGAS or STING effectively attenuates neuroinflammatory pathways.[35] NAD^+ regulates enzymes like sirtuins (SIRT1, SIRT3), which control mitochondrial biogenesis and oxidative stress.[36] Activation of the SIRT1-PGC-1α axis implies activation of antioxidant defense mechanisms, alleviating mitochondrial oxidative stress.[37] Our data revealed that NR preserved mitochondrial structure and increased levels of mitochondrial biogenesis-related factors as well as mtDNA (Fig. 3). By enhancing mitochondrial content, NR treatment improves mitochondrial function, reducing cellular stress and DNA leakage. This prevents abnormal activation of the cGAS-STING pathway. NR could reduce ROS production and improve mitochondrial functions through inducing mitophagy.[38,39] NAD^+ has also been shown to influence mitochondrial dynamics, including the balance between mitochondrial fission and fusion.[40] Whether NR helps preserve mitochondrial function and protect against retinal degeneration through the regulation of mitochondrial dynamics requires further investigation.

Microglia, activated by retinal stress, exacerbate damage through pro-inflammatory cytokines and pyroptosis (Fig. 4). Increasing evidence suggest that STING signaling exacerbates pyroptosis-associated damage and inflammasome activation in several pathological conditions.[41] Consistent with what others have reported,[42,43] the expression of pyroptosis-related cytokines increased significantly after light exposure (Fig. 5). We propose that pyroptosis is a likely consequence of microglial activation in the context of retinal degeneration, particularly following the activation of the cGAS-STING pathway in the LIRD model. When we suppressed STING expression using the selective STING inhibitor H-151, both microglial activation and pyroptosis were significantly reduced (Fig. 6), indicating that the cGAS-STING pathway is a critical mediator of retinal inflammation and photoreceptor loss.

Although NR suppressed microglia activation and subsequent inflammation, the exact role of microglia in retinal degeneration remains inconclusive. Some studies have shown that microglia can exert neuroprotective effects, as their depletion accelerates photoreceptor death in response to light damage or retinal detachment.[44,45] However, CSF1R inhibitors reduce microglial activation but may

Investigative Ophthalmology & Visual Science

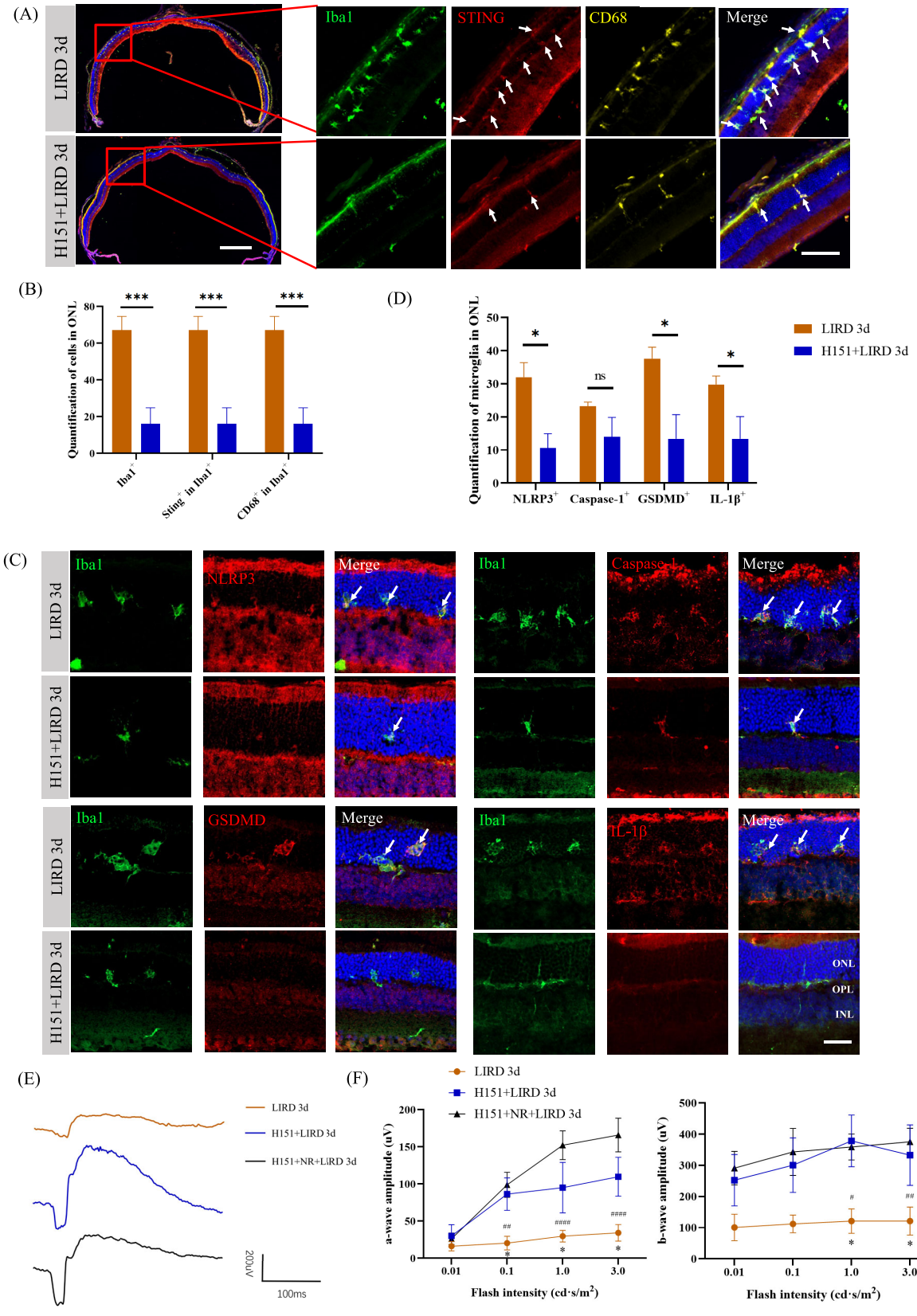

Figure 6. STING deficiency attenuated light-induced microglial activation and protected against retinal degeneration. **(A)** Representative images of entire retinal section co-stained with Iba1 (*green*), STING (*red*), and CD68 (*yellow*) from LIRD mice with or without H151 treatment. *Scale bar*: 500 µm. Magnified single-plane images were shown on the right. *Scale bar*: 100 µm. **(B)** Quantification of Iba1+ cells, STING+ Iba1+ cells, and CD68+ Iba1+ cells of each group in ONL at three days after light exposure (n = 5/group). Phagocytic microglia (CD68+ Iba1+ cells) migrated to the ONL after light exposure, whereas STING deficiency reduced light-induced migration of phagocytic microglia.

Investigative Ophthalmology & Visual Science

Arrows point to the colocalization of markers. *$P < 0.05$, **$P < 0.01$, ***$P < 0.001$, ****$P < 0.0001$, with unpaired *t*-test. **(C)** Colocalization of pyroptosis-related proteins (red) and Iba1+ microglia (green) in the retinal sections from each group. *Scale bar*: 30 µm. **(D)** Quantification of NLRP3+, Caspase-1+, GSDMD+, and IL-1β+ in Iba1+ cells in ONL at three days after light exposure ($n = 5$/group). **(E)** Representative ERG waveforms of a single eye from each group. **(F)** Scotopic ERG a-wave (*left panel*) and b-wave (*right panel*) mean amplitudes from LIRD mice treated with H151 or combination of H151 and NR ($n = 4$–5/group). Mice treated with H151 exhibited significantly higher a- and b-wave mean amplitudes (*blue line*) compared to the LIRD group (*orange line*). NR supplement (*black line*) did not add more protection to H151-treated retinas. Compared with the H151+LIRD group, *$P < 0.05$; Compared with the H151+NR+LIRD group, #$P < 0.05$, ##$P < 0.01$, ####$P < 0.0001$, by two-way ANOVA with Tukey's multiple comparisons test. *Error bars*: SEM.

not fully suppress inflammatory responses, with residual microglial or other immune cells possibly exacerbating tissue damage.[46,47] Notably, O'Koren et al.[44] further revealed that microglia in the adult retina exhibit niche-dependent functional specializations under both healthy and pathological conditions. These findings collectively suggest a complex role for microglia in retinal inflammation and photoreceptor survival, highlighting the need for tightly regulated microglial responses. Studies have shown that NR treatment could increase intracellular NAD^+ in microglia or Müller cells, thereby targeting NAD^+-consuming enzymes and leading to a reduction in the expression of NF-κB and other proinflammatory genes.[48,49] In the context of light-induced injury, whether NR treatment directly targets the NAD^+-consuming enzymes in microglia to regulate microglial activity warrants further investigation.

This study suggests the potential role of NR in inflammation regulation and mitochondrial biogenesis in a LIRD mouse model. NR supplementation has shown a favorable safety profile in clinical studies with minimal adverse effects at therapeutic doses.[50,51] NR's ability to modulate neuroinflammation could be beneficial for age-related diseases and neurodegenerative conditions where chronic inflammation and impaired NAD^+ metabolism are key factors. Future clinical trials are necessary to evaluate NR's long-term safety and efficacy.

In conclusion, NR treatment suppressed STING expression, inhibited microglial pyroptosis, and reduced retinal inflammation and photoreceptor loss, highlighting the potential of targeting the microglial cGAS-STING-pyroptosis pathway for retinal degenerative diseases.

Acknowledgments

Supported by the National Natural Science Foundation of China (No: 82201228, 82070967), the Natural Science Foundation of Hunan Province (No: 2024JJ6570) and the Natural Science Foundation of Changsha (No: kq2403080). The Scientific Research Launch Project for new employees of the Second Xiangya Hospital of Central South University.

Disclosure: **S. Zhu**, None; **L. Zhang**, None; **P. Tong**, None; **J. Chen**, None; **C. Wang**, None; **Z. Wang**, None; **J. Liu**, None; **P. Duan**, None; **Q. Jiang**, None; **Y. Zhou**, None; **G. Tan**, None; **X. Zhang**, None; **B. Jiang**, None

References

1. Fletcher EL. Mechanisms of photoreceptor death during retinal degeneration. *Optom Vis Sci*. 2010;87:269–275.
2. Gagliardi G, Ben M'Barek K, Goureau O. Photoreceptor cell replacement in macular degeneration and retinitis pigmentosa: a pluripotent stem cell-based approach. *Prog Retin Eye Res*. 2019;71:1–25.
3. Kaur G, Singh NK. The role of inflammation in retinal neurodegeneration and degenerative diseases. *Int J Mol Sci*. 2021;23:386.
4. Yoshida N, Ikeda Y, Notomi S, et al. Clinical evidence of sustained chronic inflammatory reaction in retinitis pigmentosa. *Ophthalmology*. 2013;120:100–105.
5. Man SM, Kanneganti TD. Converging roles of caspases in inflammasome activation, cell death and innate immunity. *Nat Rev Immunol*. 2016;16:7–21.
6. Shi J, Zhao Y, Wang K, et al. Cleavage of GSDMD by inflammatory caspases determines pyroptotic cell death. *Nature*. 2015;526:660–665.
7. Aachoui Y, Sagulenko V, Miao EA, Stacey KJ. Inflammasome-mediated pyroptotic and apoptotic cell death, and defense against infection. *Curr Opin Microbiol*. 2013;16:319–326.
8. Shi J, Gao W, Shao F. Pyroptosis: gasdermin-mediated programmed necrotic cell death. *Trends Biochem Sci*. 2017;42:245–254.
9. Murakami Y, Nakabeppu Y, Sonoda KH. Oxidative stress and microglial response in retinitis pigmentosa. *Int J Mol Sci*. 2020;21:7170.
10. Wong-Riley MT. Energy metabolism of the visual system. *Eye Brain*. 2010;2:99–116.
11. Okawa H, Sampath AP, Laughlin SB, Fain GL. ATP consumption by mammalian rod photoreceptors in darkness and in light. *Curr Biol*. 2008;18:1917–1921.
12. Litwiniuk A, Baranowska-Bik A, Domanska A, Kalisz M, Bik W. Contribution of mitochondrial dysfunction combined with NLRP3 inflammasome activation in selected neurodegenerative diseases. *Pharmaceuticals*. 2021;14:1221.
13. Ferrington DA, Fisher CR, Kowluru RA. Mitochondrial defects drive degenerative retinal diseases. *Trends Mol Med*. 2020;26:105–118.
14. Zhao Y, Liu B, Xu L, et al. ROS-induced mtDNA release: the emerging messenger for communication between neurons and innate immune cells during neurodegenerative disorder progression. *Antioxidants*. 2021;10:1917.
15. Wu J, Sun L, Chen X, et al. Cyclic GMP-AMP is an endogenous second messenger in innate immune signaling by cytosolic DNA. *Science*. 2013;339:826–830.
16. Gulen MF, Samson N, Keller A, et al. cGAS-STING drives ageing-related inflammation and neurodegeneration. *Nature*. 2023;620:374–380.
17. Hinkle JT, Patel J, Panicker N, et al. STING mediates neurodegeneration and neuroinflammation in nigrostriatal alpha-synucleinopathy. *Proc Natl Acad Sci USA*. 2022;119:e2118819119.
18. Amjad S, Nisar S, Bhat AA, et al. Role of NAD(+) in regulating cellular and metabolic signaling pathways. *Mol Metab*. 2021;49:101195.
19. Sasaki Y, Kakita H, Kubota S, et al. SARM1 depletion rescues NMNAT1-dependent photoreceptor cell death and retinal degeneration. *Elife*. 2020;9:e62027.
20. Lin JB, Kubota S, Ban N, et al. NAMPT-mediated NAD(+) biosynthesis is essential for vision in mice. *Cell Rep*. 2016;17:69–85.

21. Mills KF, Yoshida S, Stein LR, et al. Long-term administration of nicotinamide mononucleotide mitigates age-associated physiological decline in mice. *Cell Metab*. 2016;24:795–806.
22. Zhang X, Henneman NF, Girardot PE, et al. Systemic treatment with nicotinamide riboside is protective in a mouse model of light-induced retinal degeneration. *Invest Ophthalmol Vis Sci*. 2020;61:47.
23. Zhu X, Liu W, Tang X, et al. The BET PROTAC inhibitor dBET6 protects against retinal degeneration and inhibits the cGAS-STING in response to light damage. *J Neuroinflammation*. 2023;20:119.
24. Lam J, Katti P, Biete M, et al. A universal approach to analyzing transmission electron microscopy with ImageJ. *Cells*. 2021;10:2177.
25. Rosa JGS, Disner GR, Pinto FJ, Lima C, Lopes-Ferreira M. Revisiting retinal degeneration hallmarks: insights from molecular markers and therapy perspectives. *Int J Mol Sci*. 2023;24:13079.
26. Zong Y, Li H, Liao P, et al. Mitochondrial dysfunction: mechanisms and advances in therapy. *Signal Transduct Target Ther*. 2024;9:124.
27. Duarte JN. Neuroinflammatory mechanisms of mitochondrial dysfunction and neurodegeneration in glaucoma. *J Ophthalmol*. 2021;2021:4581909.
28. Kang I, Chu CT, Kaufman BA. The mitochondrial transcription factor TFAM in neurodegeneration: emerging evidence and mechanisms. *FEBS Lett*. 2018;592:793–811.
29. Ablasser A, Chen ZJ. cGAS in action: expanding roles in immunity and inflammation. *Science*. 2019;363(6431):eaat8657.
30. Maekawa H, Inoue T, Ouchi H, et al. Mitochondrial damage causes inflammation via cGAS-STING signaling in acute kidney injury. *Cell Rep*. 2019;29:1261–1273.e1266.
31. Gao P, Ascano M, Wu Y, et al. Cyclic [G(2′,5′)pA(3′,5′)p] is the metazoan second messenger produced by DNA-activated cyclic GMP-AMP synthase. *Cell*. 2013;153:1094–1107.
32. Anderson FL, von Herrmann KM, Andrew AS, et al. Plasma-borne indicators of inflammasome activity in Parkinson's disease patients. *NPJ Parkinsons Dis*. 2021;7:2.
33. Bergsbaken T, Fink SL, Cookson BT. Pyroptosis: host cell death and inflammation. *Nat Rev Microbiol*. 2009;7:99–109.
34. Kim J, Kim HS, Chung JH. Molecular mechanisms of mitochondrial DNA release and activation of the cGAS-STING pathway. *Exp Mol Med*. 2023;55:510–519.
35. Jiang GL, Yang XL, Zhou HJ, et al. cGAS knockdown promotes microglial M2 polarization to alleviate neuroinflammation by inhibiting cGAS-STING signaling pathway in cerebral ischemic stroke. *Brain Res Bull*. 2021;171:183–195.
36. Covarrubias AJ, Perrone R, Grozio A, Verdin E. NAD(+) metabolism and its roles in cellular processes during ageing. *Nat Rev Mol Cell Biol*. 2021;22:119–141.
37. Liang D, Zhuo Y, Guo Z, et al. SIRT1/PGC-1 pathway activation triggers autophagy/mitophagy and attenuates oxidative damage in intestinal epithelial cells. *Biochimie*. 2020;170:10–20.
38. Hou Y, Wei Y, Lautrup S, et al. NAD(+) supplementation reduces neuroinflammation and cell senescence in a transgenic mouse model of Alzheimer's disease via cGAS-STING. *Proc Natl Acad Sci USA*. 2021;118(37):e2011226118.
39. Wei Q, Hu W, Lou Q, Yu J. NAD+ inhibits the metabolic reprogramming of RPE cells in early AMD by upregulating mitophagy. *Discov Med*. 2019;27:189–196.
40. Hu L, Guo Y, Song L, et al. Nicotinamide riboside promotes Mfn2-mediated mitochondrial fusion in diabetic hearts through the SIRT1-PGC1alpha-PPARalpha pathway. *Free Radic Biol Med*. 2022;183:75–88.
41. Sun F, Liu Z, Yang Z, Liu S, Guan W. The emerging role of STING-dependent signaling on cell death. *Immunol Res*. 2019;67:290–296.
42. Yu X, Peng J, Zhong Q, Wu A, Deng X, Zhu Y. Caspase-1 knockout disrupts pyroptosis and protects photoreceptor cells from photochemical damage. *Mol Cell Probes*. 2024;78:101991.
43. Zhang Y, Zhao Z, Zhao X, et al. HMGB2 causes photoreceptor death via down-regulating Nrf2/HO-1 and up-regulating NF-kappaB/NLRP3 signaling pathways in light-induced retinal degeneration model. *Free Radic Biol Med*. 2022;181:14–28.
44. O'Koren EG, Yu C, Klingeborn M, et al. Microglial Function Is Distinct in Different Anatomical Locations during Retinal Homeostasis and Degeneration. *Immunity*. 2019;50:723–737.e727.
45. Okunuki Y, Mukai R, Pearsall EA, et al. Microglia inhibit photoreceptor cell death and regulate immune cell infiltration in response to retinal detachment. *Proc Natl Acad Sci USA*. 2018;115:E6264–E6273.
46. Torres L, Danver J, Ji K, et al. Dynamic microglial modulation of spatial learning and social behavior. *Brain Behav Immun*. 2016;55:6–16.
47. Elmore MR, Najafi AR, Koike MA, et al. Colony-stimulating factor 1 receptor signaling is necessary for microglia viability, unmasking a microglia progenitor cell in the adult brain. *Neuron*. 2014;82:380–397.
48. Terao R, Lee TJ, Colasanti J, et al. LXR/CD38 activation drives cholesterol-induced macrophage senescence and neurodegeneration via NAD(+) depletion. *Cell Rep*. 2024;43:114102.
49. Lin R, Yu J. The role of NAD(+) metabolism in macrophages in age-related macular degeneration. *Mech Ageing Dev*. 2023;209:111755.
50. Martens CR, Denman BA, Mazzo MR, et al. Chronic nicotinamide riboside supplementation is well-tolerated and elevates NAD(+) in healthy middle-aged and older adults. *Nat Commun*. 2018;9:1286.
51. Mehmel M, Jovanovic N, Spitz U. Nicotinamide riboside-the current state of research and therapeutic uses. *Nutrients*. 2020;12.

Investigative Ophthalmology & Visual Science